

Accretion of gas onto nearby spiral galaxies

F. Fraternali^{1*} and J. J. Binney²

¹*Department of Astronomy, University of Bologna, via Ranzani 1, 40127, Bologna, Italy*

²*Rudolf Peierls Centre for Theoretical Physics, 1 Keble Road, Oxford, OX1 3NP, UK*

Accepted xxx. Received xxx

ABSTRACT

We present evidence for cosmological gas accretion onto spiral galaxies in the local universe. The accretion is seen through its effects on the dynamics of the extra-planar neutral gas. The accretion rates that we estimate for two nearby spiral galaxies are of the order of their star formation rates. Our model shows that most of the extra-planar gas is produced by supernova feedback (galactic fountain) and only 10 – 20% comes from accretion. The accreting material must have low specific angular momentum about the disc’s spin axis, although the magnitude of the specific angular-momentum vector can be higher. We also explore the effects of a hot corona on the dynamics of the extra-planar gas and find that it is unlikely to be responsible for the observed kinematical pattern and the source of accreted gas. However, the interaction with the fountain flow should profoundly affect the hydrodynamics of the corona.

Key words: galaxies: kinematics and dynamics galaxies: individual: NGC 891, NGC 2403 galaxies: haloes galaxies: evolution ISM: kinematics and dynamics

1 INTRODUCTION

Observations of several spiral galaxies have revealed thick HI layers or HI haloes surrounding the galactic discs (e.g. Swaters, Sancisi & van der Hulst 1997; Fraternali et al. 2002; Matthews & Wood 2003). The kinematics of this extra-planar gas is characterized by: (i) a decrease in rotation velocity v_ϕ in the vertical direction (Swaters, Sancisi & van der Hulst 1997; Fraternali et al. 2005); (ii) vertical motions from and towards the disc (Boomsma 2007); (iii) a general radial inflow (Fraternali et al. 2001). In a previous paper (Fraternali & Binney 2006, hereafter FB06) we developed the galactic fountain model of extra-planar HI in which gas clouds are shot upwards from regions of star formation in the disc, and then follow ballistic trajectories before returning to the disc (see also Collins, Benjamin & Rand 2002). Comparing the predictions of this model with data from deep HI surveys of the edge-on galaxy NGC 891 and the moderately inclined galaxy NGC 2403 we concluded that the model fails in two respects: (i) it under-predicts the difference between the rotation rates of disc and extra-planar gas, and (ii) it predicts that the extra-planar gas should on average be flowing out rather than in. We showed that these failures could not be rectified by assuming that the clouds were visible in the 21-cm line on only part of their trajectories.

In this paper we extend the fountain model to include

interaction with extragalactic gas. This gas is expected to take two forms: (i) the hot corona of gas at the virial temperature, and (ii) cold, infalling clouds. Standard cosmological models of galaxy formation imply the existence of both types of gas. In fact, arguments based on the cosmic background radiation and primordial nucleosynthesis, combined with the measured baryonic masses of galaxies imply that most of the baryons in the Universe must lie in extragalactic gas (e.g. White & Frenk 1991; Sommer-Larsen 2006). Limits on the background radiation levels at frequencies from the X-ray to radio bands imply that most of the gas must be at low densities and hot, $T \gtrsim 10^6$ K. From the existence of Ca II absorption lines in the spectra of stars at high Galactic latitudes, Spitzer (1956) inferred the existence of such gas around the Milky Way, and by mapping the soft X-ray emission from the massive galaxy NGC 5746 Pedersen et al. (2006) have established the existence of such gas around at least some galaxies. Benjamin & Danly (1997) showed that observed HI clouds of fountain gas will experience appreciable drag as they move through the coronal gas. The head-tail morphology of many compact high-velocity clouds around the Milky Way (Brüns et al. 2001) confirms this prediction. In this paper we add this drag to our earlier dynamical model and show that although it cannot account for the observed velocities of extra-planar HI, it must have major implications for the hydrodynamics of the coronal gas.

The existence of streams of cold gas around galaxies is less securely established, but is supported by several lines of argument. From a theoretical perspective, extended Press-

* E-mail: filippo.fraternali@bo.astro.it

Schechter theory (Bond et al. 1991; Lacey & Cole 1993) predicts that galaxies grow through a series of infall events. These range from a small number of major mergers, right down to an almost continuous drizzle of infalling dwarf galaxies and gas clouds. It is hard to assess the importance of this drizzle from numerical simulations of limited mass and spatial resolution, but as simulations have become more sophisticated, awareness of the importance of the drizzle has increased (Birnboim & Dekel 2003; Keres et al. 2005; Semelin & Combes 2005; Dekel & Birnboim 2006).

The rate of star-formation in the solar neighborhood has been remarkably constant over the Galaxy’s life (Twarog 1980; Binney, Dehnen & Bertelli 2000), which suggests that the gas density has not decreased significantly even though the current star-formation rate would exhaust the gas in a couple of gigayears. These facts strongly suggest that gas consumed by star formation is mostly replaced by accretion, whether by cooling of the corona or cold infall. Steady accretion of metal-poor gas would also explain the discrepancy between the observed stellar metallicity distribution in the solar neighbourhood and that predicted by the closed-box model of chemical evolution (Tinsley 1981; Matteucci 2003).

What remains unclear is whether gas is predominantly accreted from the hot corona or comes by cold infall, and in the latter case, how important is steady drizzle compared to the acquisition of gas in parcels associated with discrete events such as the capture of the Sagittarius dwarf galaxy. In our Galaxy, a limit can be placed on the masses of infalling objects because the solar neighbourhood, which is both old (Binney, Dehnen & Bertelli 2000) and cold, would be rapidly heated by the passage through it of objects with masses $\gtrsim 10^7 M_\odot$ (Lacey & Ostriker 1985; Toth & Ostriker 1992).

An observational indication of the importance of cold infall is the fact that the Galaxy is surrounded by a large number of clouds, the so-called high-velocity clouds (HVCs) (Wakker & van Woerden 1997) that can be observed in HI and on the average have negative radial velocities. New distance estimates for the large HVC complexes show that they are located in the upper halo of the Milky Way and have masses of order $10^{6-7} M_\odot$ (Wakker et al. 2007a, 2008). Most HVCs are too far from the plane to be part of the Galactic fountain, and those that have measured metallicities are too metal-poor to be predominantly gas ejected from the star-forming disc (Tripp et al. 2003). The net infall rate \dot{M} associated with high-velocity clouds seems to be $\dot{M} \sim 0.2 M_\odot \text{ yr}^{-1}$ (Wakker et al. 2007a; Peek, Putman & Sommer-Larsen 2007), which is about an order of magnitude lower than the SFR of the Milky Way.

There are observations of infalling gas complexes also in external galaxies (for a review see Sancisi et al. 2008). A well known example is the massive HI complex accreted by M 101 (van der Hulst & Sancisi 1988) but the majority of these accreting clouds will have much lower masses and have escaped detection. In fact, new deep observations of the region of space around M 31 reveals the presence of numerous HVCs with masses down to a few $10^4 M_\odot$ (Westmeier, Braun, & Thilker 2005). In some cases, halo clouds are detected at very anomalous (*counter-rotating*) velocities with respect to the disc rotation and massive cold filaments are also observed (Oosterloo, Fraternali & Sancisi 2007;

Fraternali et al. 2002). Gas accretion may be also arise from interactions with satellite galaxies (van der Hulst & Sancisi 2005; Sancisi et al. 2008).

The above data suggest that star forming galaxies are accreting material from the intergalactic space at a rate of at least $\dot{M} \sim 0.2 M_\odot \text{ yr}^{-1}$ (Sancisi et al. 2008) which is typically 10 – 20% of the SFR for these objects. In this paper we argue that this directly observed accretion rate is in fact a lower limit. Most of the accreting gas interacts with gas pushed up into the halo by stellar feedback, and it is *observable* only indirectly via the peculiar kinematics of the extra-planar gas.

2 THE MODEL

Our pure fountain model is described in Fraternali & Binney (2006). We integrate orbits of particles that are ejected from the disc of a spiral galaxy and travel through the halo until they fall back to the disc. The data require that the particles are ejected nearly straight upwards. The kinetic energy of ejection is $\lesssim 4$ percent of the mechanical energy produced by supernovae. The potential of the galaxy comprises the contributions of four components: stellar and gaseous discs, both described by exponential profiles, a dark matter (DM) halo and a bulge, both described by double power law profiles (Dehnen & Binney 1998). The potential is constrained by the HI rotation curve (Oosterloo, Fraternali & Sancisi 2007; Fraternali et al. 2002). After each timestep of the orbit integrations, the positions and velocities of the particles are projected along the line of sight to produce an artificial cube of positions on the sky and radial velocities. This cube is then smoothed and compared with the observed HI data cubes. Typically, the mass and spatial resolutions of the simulations are two orders of magnitude higher than those of the data, therefore the global effect is that of a smooth fountain flow (see also FB06).

3 INTERACTION WITH THE HOT CORONA

In this section we concentrate on the edge-on galaxy NGC 891, for which parameters of the corona can be obtained from X-ray observations (Bregman & Houck 1997; Strickland et al. 2004). We model the corona as a plasma of temperature T that is in equilibrium in the axisymmetric potential of the galaxy $\Phi(R, z)$. Then the hydrostatic equations in cylindrical coordinates imply that the density is

$$\rho(R, z) = A \exp \left[-\frac{\mu m_p}{kT} \left(\Phi(R, z) - \frac{v_0^2}{2} \right) \right], \quad (1)$$

where A is a constant, $\mu = 0.61$ is the molecular weight of the plasma, and v_0 is the speed at which the corona rotates (assumed to be independent of radius). We adopt the temperature $T = 2.7 \times 10^6$ K determined from X-ray spectra by Strickland et al. (2004) and for several values of v_0 determine A by fitting the predicted X-ray luminosity L_X to that observed. L_X was obtained by integrating the emission predicted by equation (1) over roughly the same regions as that of the X-ray observations. The emissivity was taken from the MEKAL recipe (Mewe, Lemen & Oord 1986;

Liedahl, Osterheld & Goldstein 1995) that is embedded in the XSPEC package.

The X-ray distribution is not highly flattened, so the adopted values of v_0 lie significantly below the local circular speed.

In reality a significant fraction of the observed X-ray luminosity will arise from interfaces between cold clouds and the corona rather than from the main body of the corona. Consequently, our procedure for determining A will tend to overestimate the corona's density. This fact will reinforce the conclusion reached below, that the corona cannot absorb angular momentum fast enough to account for the observed rotational lag of the HI halo.

3.1 Cloud dynamics

We consider the motion of an HI cloud with temperature $\lesssim 10^4$ K through the corona. Near the disc, the corona's cooling time $t_{\text{cool}} = m_p kT / (\Lambda\rho)$ is $\gtrsim 100$ Myr, which is much longer than the flow time

$$t_{\text{flow}} = D/v \sim 1 \text{ Myr} \quad (2)$$

around a cloud of diameter $D \sim 100$ pc at speed $v \sim 100 \text{ km s}^{-1}$, so most of the coronal gas is expected to pass right by, and we should idealize the interaction as the flow of a gas around a dense object. The densities of the cloud and the corona differ by a factor $\gtrsim 300$, so the motion is akin to the flight through air of water drops from a garden sprinkler.

We assume that the flow of the corona past a cloud has a high Reynolds number; this assumption minimizes the drag on the cloud, and we shall see that even this minimum drag is highly significant. When the Reynolds number is high, the drag is proportional to the square of the flow velocity v of the corona past the cloud, so the acceleration of the cloud can be written

$$\vec{g}_D(R, z) = -\frac{Cv}{L}\vec{v}, \quad (3)$$

where C is a dimensionless constant of order unity, and L is the distance over which the cloud interacts with its own mass of coronal gas:

$$L = \frac{m}{\rho\sigma}, \quad (4)$$

with σ and m the cloud's cross-sectional area and mass, respectively. In the absence of other forces, drag causes the cloud's velocity to decay as

$$\vec{v}(t) = \frac{\vec{v}_0}{1 + Ct v_0 / L}. \quad (5)$$

Thus the speed halves in a time $t_{\text{drag}} = L / (Cv_0) \simeq 300 t_{\text{flow}}$. For $v_0 \sim 100 \text{ km s}^{-1}$, $t_{\text{drag}} \sim 300$ Myr is of the same order as the orbital times of the clouds that make up the HI halo (FB06 Fig. 10). For low Reynolds numbers, t_{drag} would be even lower than the above estimate. Note that if a cloud were to sweep up all the coronal gas that it encounters rather than deflecting it, the drag on a cloud would be still given by equations (3) and (4).

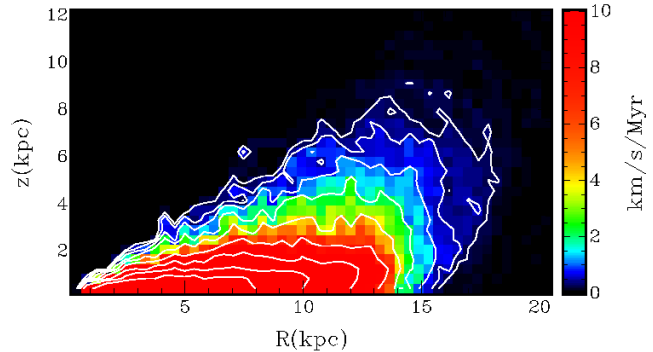


Figure 1. Azimuthal velocities acquired by the hot corona per Myr due to the transferring of angular momentum from the fountain gas. From outside in contours are at 0.25, 0.5, 1, 2, 4, 8, 16, 32, 64 $\text{km s}^{-1}/\text{Myr}$.

3.2 Coronal spinup

Since these numbers establish that momentum transfer between clouds and coronal gas may be a significant process, consider the possibility that this process produces the additional lag of the HI halo relative to the disc that FB06 found the observations to require. Let fountain gas be ejected at a rate \dot{M}_f and let $\delta\ell$ be the amount by which its specific angular momentum is reduced by interaction with the corona. Then the rate at which the corona absorbs angular momentum is $\dot{L} = \dot{M}_f \delta\ell$, and the time required for the corona to be spun up to near the circular speed is

$$t_{\text{spin}} = \frac{M_{\text{corona}} \ell_c}{\dot{M}_f \delta\ell}, \quad (6)$$

where $\ell_c = Rv_c$ is the specific angular momentum of a circular orbit.

Considering just the HI that is more than 1.3 kpc from the plane, FB06 found that $\delta\ell/\ell_c \sim 0.05$ and $\dot{M}_f = 10^7 M_\odot \text{ Myr}^{-1}$, so $t_{\text{spin}} \sim (2M_{\text{corona}}/10^6 M_\odot) \text{ Myr}$. The mass of the corona inside radius r is $3 \times 10^7 (r/10 \text{ kpc}) M_\odot$, so $t_{\text{spin}} \sim 60 (r/10 \text{ kpc}) \text{ Myr}$. That is, the capacity of the corona for absorbing angular momentum is so slight that it will be brought to corotation with the HI halo within a dynamical time unless the angular momentum is moved from the radii ~ 10 kpc at which it is imparted to much larger radii. This cannot be done in less than a dynamical time.

To test this conclusion, we added the deceleration (3) to the fountain model presented in FB06 – a description of the initial parameters of the model can be found in FB06. Here the potential is taken to be the one appropriate to a maximum disc, but in FB06 we showed that the kinematics of the extra-planar gas is insensitive to the choice of potential. As determined in FB06, the total mass of the HI halo is $M_{\text{halo}} = 2 \times 10^9 M_\odot$.

We adjusted the ratio m/σ until the model reproduced the observed lag velocity. We considered hot coronas rotating at different speeds and with different velocity patterns. In the case of a corona that rotates at 100 km s^{-1} independent of radius, the data for NGC 891 are successfully simulated when $m/\sigma \approx 10^5 M_\odot \text{ kpc}^{-2}$ (see also Fraternali et al. 2007).

However, in this picture, in which the coronal gas simply flows around clouds without being accreted onto them, all

the angular momentum lost by the HI clouds of the halo has to be absorbed by the corona. If angular momentum taken up by the corona in an annulus centred on (R, z) remains in that annulus, then in 1 Myr the azimuthal velocity of the corona at (R, z) will increase by the amounts plotted in Fig. 1; we see that the spin-up time of the inner corona is extremely short; within a time $t_{\text{spin}} \approx 10$ Myr the inner corona will co-rotate with the disc and the drag will vanish.

Thus the corona can be responsible for the observed rotational lag of the HI halo only if the clouds sweep up the coronal gas along their path rather than deflecting it, which is not expected to happen given the large ratio of the cooling time of coronal gas to the flow time around a cloud. If clouds do not sweep up coronal gas, and the ratio m/σ is not much larger than the above estimate, the HI halo will stir the corona rather like the impeller of a centrifugal pump stirs the fluid in the pump. In response to this stirring, the coronal gas will move rapidly outwards parallel to the disc plane, and be replaced by gas that moves down parallel to the symmetry axis. Thus the HI halo must drive a large-scale circulation in the corona. Calculation of the dynamics of this circulation lies beyond the scope of this paper, but is a topic that needs to be pursued because it must have significant implications for the corona and X-ray observations.

4 SWEEPING UP OF AMBIENT GAS

In light of the conclusion above that the hot corona can be responsible for the observed rotational lag only if it is swept up by fountain clouds, we now examine the case in which fountain clouds sweep up ambient gas. Given the long cooling time of the coronal gas, we envisage that the bulk of the gas swept up is cold, infalling material. When a fountain cloud impacts on a stream of cold gas, some material is likely to be heated to the virial temperature, but given the high densities involved, and the potential for rapid turbulent mixing of the two bodies of gas, other material will be swept up into the cloud of fountain gas. For simplicity we assume that this is the dominant process. That is, we assume that a travelling cloud of mass m gains mass at a rate $\dot{m} = \alpha m$ and momentum at a rate $\dot{m}\vec{v}_i$, where \vec{v}_i is the velocity of the infalling material. We implement these assumptions by modifying the procedure used in FB06 to determine the trajectories of clouds as follows. After each timestep of duration δt we increment the cloud's mass by $\delta m = \alpha m \delta t$ and change its velocity from \vec{v}_0 to

$$\vec{v}_1 = \frac{m_0 \vec{v}_0 + \delta m \vec{v}_i}{m_0 + \delta m}, \quad (7)$$

where \vec{v}_i is the velocity of the infalling material.

The parameter α , which is proportional to the volume density of infalling material, becomes the key parameter to be constrained by the data. Its spatial variation $\alpha(R, z)$ is not known. However, experimenting with different patterns we found that the results are not qualitatively very different as long as its value does not vary too steeply in the inner halo. We therefore take α to be constant, which implies that in a given interval δt a cloud captures the same amount of infalling gas regardless of its location. We exclude regions very close to the disc, $|z| < 0.2$ kpc.

A more critical characteristic of infalling material is the velocity \vec{v}_i at which it is captured. At any given time infalling material is likely to have some non-vanishing average angular momentum, but the direction of this average changes over time (Quinn & Binney 1992; Aubert, Pichon & Colombi 2004), and we neglect the correlation between its average value at the present time and the angular-momentum vector of the disc.

We consider two extreme possibilities: one possibility is that the z component of \vec{v}_i is dominant and negative, implying that infall is predominantly parallel to the z axis. The modulus of v_{iz} is chosen at random between zero and the local escape speed. The other two components of \vec{v}_i are taken to follow Gaussian distributions with zero mean and dispersion $\sim 50 \text{ km s}^{-1}$. The magnitude of \vec{v}_i is constrained to be less than the escape speed. With this prescription, the angular momentum about the z axis of an infalling cloud vanishes in the mean.

The second possibility considered is that the dominant component of \vec{v}_i is parallel to the local radius vector. For this component we use the distribution that was previously used for v_{iz} . The two tangential components of \vec{v}_i are drawn from a Gaussian distribution with dispersion $\sim 50 \text{ km s}^{-1}$, again subject to the constraint that the total speed should not exceed the escape speed. This prescription may be motivated by the observation that in cosmological simulations infalling material is typically on highly eccentric orbits (Knebe et al. 2004). On such an orbit, the radial component of the velocity vector is usually dominant. We also considered models with random velocity components and no preferred directions; these gave results in between the two extreme possibilities described here.

4.1 Application to NGC 891

We applied our model of a fountain that interacts with infalling gas to the HI observations of NGC 891 (Oosterloo, Fraternali & Sancisi 2007). As in FB06, clouds were ejected nearly vertically from the disc with a velocity drawn from a Gaussian distribution, and the dispersion of this distribution was adjusted to optimize the agreement between the model and observational data cubes.

Fig. 2 (leftmost column) shows five sample channel maps for NGC 891 at $28''$ (about 1.3 kpc) resolution; heliocentric velocities in km s^{-1} are in the top-left corners. A key feature of the data is that the apparent vertical thickness of the channel maps increases as the velocity moves away from values characteristic of fast rotation towards the systemic velocity. Thus in the $v_{\text{hel}} = 292 \text{ km s}^{-1}$ channel the HI appears thin, and in the $v_{\text{sys}} = 528 \text{ km s}^{-1}$ channel it has a very extended vertical distribution. This behaviour reflects the lag of the HI halo with respect to the disc and is the main constraint on our models.

In the rightmost column of the same Fig. 2 we report the prediction from a model in which the extra-planar gas is produced by stellar feedback only (pure galactic fountain), presented in FB06. Note that, thanks to the availability of a new deeper data cube (Oosterloo, Fraternali & Sancisi 2007) a lower contour is shown than appears in FB06. These upper model maps show the distribution of HI to be much thicker than is found in the observed channel maps on the extreme left. This mismatch arises because in the model of

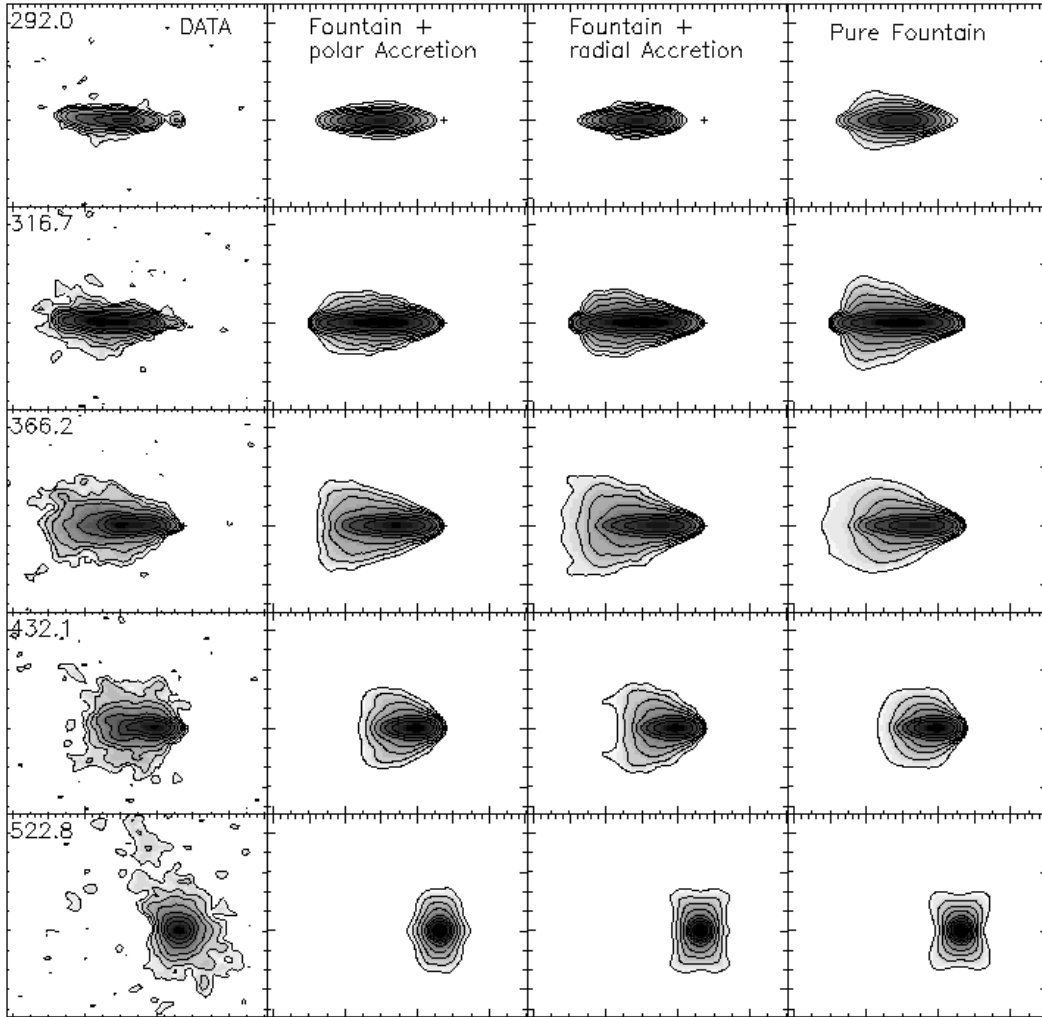


Figure 2. Comparison between 5 channel maps for NGC 891 (Oosterloo, Fraternali & Sancisi 2007) and those obtained with three dynamical models. The first column shows the data, heliocentric radial velocities (in km s^{-1}) are reported in the upper left corners. The channel map in the bottom row is roughly at the systemic velocity ($V_{\text{sys}} = 528 \text{ km s}^{-1}$). Contour levels (for data and models) are: 0.25 (2.5σ), 5, 1, 2, 5, 10, 20, 50 mJy beam^{-1} .

Table 1. Fountain + accretion models for NGC 891

Model	Phase change	h_v (km s^{-1})	α (Gyr^{-1})	\dot{M}_{in} ($M_{\odot} \text{ yr}^{-1}$)	$\frac{\dot{M}_{\text{in}}}{\dot{M}_{\text{out}}}$
Polar	no	90	2.0	3.4	0.12
Radial	yes	80	0.6	2.3	0.05

FB06 the rotation velocity decreases too slowly with increasing z . FB06 show that this problem cannot be eliminated by using different initial conditions or supposing that the gas is invisible in the first part of its orbit (phase-change models).

Consider now the models shown in the two central columns of Fig. 2. In these models the clouds of the fountain interact with an accretion flow as described above, and differ from each other in the dominant component of the infall velocity \vec{v}_i : in the left column $v_{i,z}$ is dominant, while in the right column $v_{i,r}$ dominates. The specific accretion rates are

$\alpha = 2 \text{ Gyr}^{-1}$ and $\alpha = 0.6 \text{ Gyr}^{-1}$ respectively for the two models (see Table 1)

It is evident that the top two channel maps of the left-central column have narrower vertical distributions than are obtained without infalling gas, and thus provide much better fits to the data. Modest improvements in the shape of the lower two channel maps for velocities near systemic are also evident. We find that the total accretion rate of cold gas required by the model with dominant polar component of accretion is $\dot{M}_{\text{inflow}} \simeq 3.4 M_{\odot} \text{ yr}^{-1}$, which is very close to the star formation rate of NGC 891 ($\text{SFR} = 3.8 M_{\odot} \text{ yr}^{-1}$; Popescu et al. 2004).

When the dominant component of the infall velocity is radial, the data are best fitted when the fountain gas suffers a phase change such that it becomes visible as HI when $|z|$ peaks. A galaxy with the star-formation rate of NGC 891 produces a significant flux of ionizing radiation and it is plausible that a large fraction of the outgoing fountain flow would be ionised. The right-central column shows channel maps for a model in which cold material is accreting at a

rate $\dot{M}_{\text{inflow}} \simeq 2.3 M_{\odot} \text{ yr}^{-1}$. We see that this model fits the data as well as the model with polar accretion shown in the left-central column.

The two accretion models presented here are best fits to the data obtained via a minimization of the residuals between the data and the models, much as described in FB06 except that here the discrepancies are also considered channel by channel to the whole data cube and not only in the total HI maps. Once the mass of the halo has been fixed ($M_{\text{halo}} = 2 \times 10^9 M_{\odot}$), the key parameters are the accretion parameter α (related to the accretion rate \dot{M}_{inflow}) and, as in the pure fountain model, the characteristic kick velocity. For the latter we found values slightly higher than in the pure fountain model ($80\text{--}90 \text{ km s}^{-1}$) because to reach a given height fountain gas has to overcome drag from infalling gas in addition to the galaxy's gravitational field. The total energy input from the disc required to produce such a fountain flow is $\lesssim 6$ ($\lesssim 8$ for the phase change model) per cent of the energy available from the supernovae. These percentages are a factor ~ 1.5 larger than those of the pure fountain model (FB06). The actual value of the supernova feedback in galaxies is uncertain; our values agree with the prediction of hydrodynamical models (e.g. Mac Low & Ferrara 1999). The inflowing (accretion) is only ~ 10 percent of the outflowing (fountain) gas (see Table 1).

In the model with radial accretion and phase change the accretion rate is not well constrained and the data allow for values of α between 0.2 and 1.5 Gyr^{-1} . This is not surprising since this phase-change model produces a fairly good fit to the data of NGC891 also without accretion, as shown in FB06. However in the case of low accretion rate it fails completely to reproduce the inflow pattern observed in NGC 2403. We show in the next section that the inclusion of accretion elegantly solves this problem.

In the above models we assumed that the angular momentum of the accreting material about the disc's spin axis, L_z , is zero on average. We have tested whether this is a necessary requirement for the model and found that the data allow for a non-negligible L_z . At radius R the material accreting on a disc with circular speed v_c must have on average $L_z < \frac{1}{2} R v_c$. If $L_z = \frac{1}{2} R v_c$, the accretion rate required to reproduce the data becomes $\dot{M}_{\text{inflow}} \sim 6 M_{\odot} \text{ yr}^{-1}$. We discuss the implications of this requirement in Section 6.

Fraternali et al. (2005) determined the rotation speed v_{rot} of gas in NGC 891 at several heights above the plane by identifying the terminal velocity $v_{\text{term}}(R, z)$ at each position (R, z) . The rotation speed is taken to be $v_{\text{rot}} = v_{\text{term}} - \sqrt{\sigma_{\text{ran}}^2 + \sigma_{\text{obs}}^2}$, where σ_{ran} is the random velocity of HI clouds and $\sigma_{\text{obs}} = 6 \text{ km s}^{-1}$ is the observational error. Fraternali et al. (2005) assumed that $\sigma_{\text{ran}} \simeq 8 \text{ km s}^{-1}$ everywhere. More recent modelling shows clear evidence for a larger dispersion $\sigma_{\text{ran}} \simeq 20 \text{ km s}^{-1}$ away from the plane (Oosterloo, Fraternali & Sancisi 2007). So it is appropriate to move the points from Fraternali et al. (2005) down by $11 \text{ km s}^{-1} = \sqrt{20^2 + 6^2} - \sqrt{8^2 + 6^2}$ (details in Fraternali, in prep.); the data points in Fig. 3 show the corrected points for $z = 3.9$ and $z = 5.2 \text{ kpc}$. The lines show model predictions obtained from weighted means of the azimuthal components of the particle velocities. We see that the model with infall (full/blue curves) fits the data points very well, while the

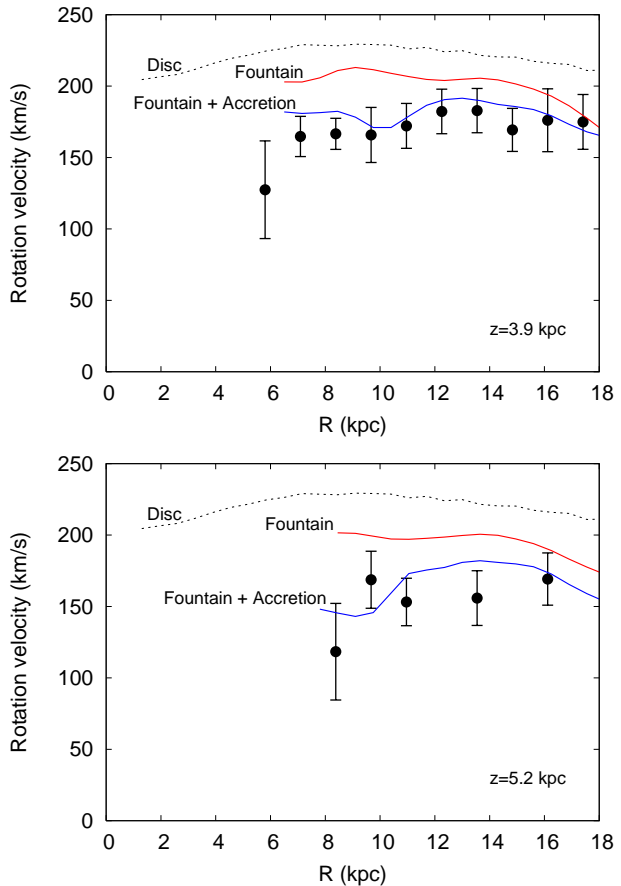


Figure 3. Rotational velocities (points) obtained from the HI data at 3.9 kpc (upper panel) and 5.2 kpc (lower panel) from the plane of NGC 891 (Fraternali et al. 2005). The dotted line shows the rotation curve in the plane, while the other two lines show the azimuthal velocity predicted by our pure fountain (dotted-dashed/red) and fountain+accretion (solid/blue) models.

pure fountain model (dashed/red curves) yields only half the lag required by the data.

4.2 Application to NGC 2403

Consider now the ability of the model that includes infall to reproduce the data for the moderately inclined galaxy NGC 2403. Fraternali et al. (2002) showed that the HI measurements of this galaxy reveal an extended layer of extraplanar gas that rotates less rapidly than the disc gas and flows in towards the centre of the galaxy. In FB06 we showed that pure fountain models in which the halo gas rotates less fast than the disc show outflow rather than inflow. Here we show that adding accretion similar to that derived for NGC 891 causes the model to predict inflow similar to that observed in NGC 2403.

Fig. 4 shows position-velocity plots along the minor axis of NGC 2403 (middle row) and parallel to this axis at offsets of $\pm 2'$. The leftmost column shows the data, the rightmost column the pure fountain model and the middle column the fountain with accretion. Similar results are obtained regardless of whether the accretion has a polar or radial pattern, and in the latter case a phase change is not required (see Ta-

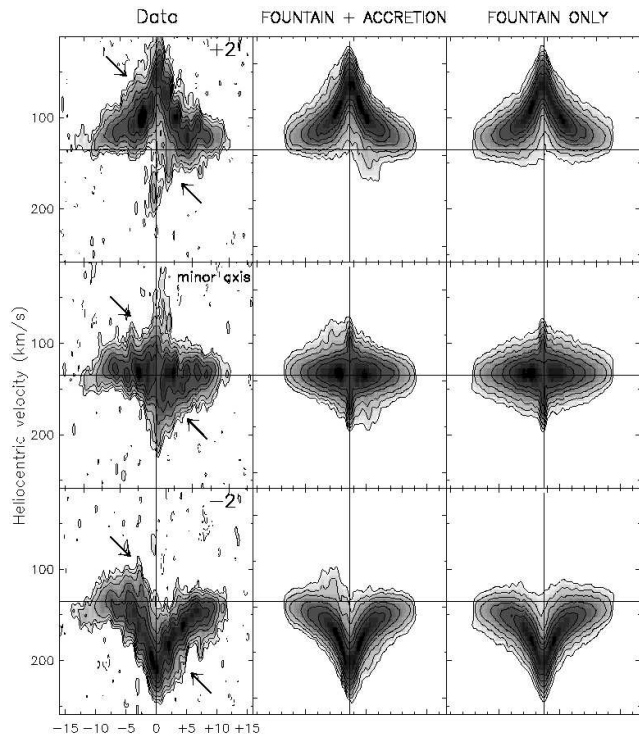


Figure 4. Comparison between 3 p-V plots parallel to the minor axis of NGC 2403 and those obtained with two dynamical models. The first column shows the data, contour levels (for data and models) are 0.5 ($\sim 2.5\sigma$), 1, 2, 5, 10, 20, 50 mJy beam $^{-1}$.

Table 2. Fountain+accretion models for NGC 2403

Model	Phase change	h_v (km s $^{-1}$)	α (Gyr^{-1})	\dot{M}_{inflow} ($M_{\odot} yr^{-1}$)	$\frac{\dot{M}_{in}}{\dot{M}_{out}}$
Polar	no	55	2.0	1.0	0.21
Radial	no	50	1.2	0.6	0.15

ble 2). The results shown are obtained for the same values of the accretion parameter α as was derived from NGC 891 (for the radial infall model we doubled the value of α since clouds are now visible along the whole trajectory). We see that the model with infall reproduces the data quite well. The required accretion rate is $\dot{M}_{inflow} \approx 0.8 M_{\odot} yr^{-1}$. For comparison the SFR in NGC 2403 is $1.2 M_{\odot} yr^{-1}$ (Kennicutt et al. 2003).

Fraternali et al. (2001) have separated the so-called anomalous (extra-planar) gas in NGC 2403 from the disc gas with a technique described in Fraternali et al. (2002). The resulting velocity field of the extra-planar gas (here shown in Fig. 5, upper panel) shows a clear sign of radial inflow in that the kinematical minor axis is rotated counter-clockwise and not orthogonal to the major axis. We have used the same procedure to derive velocity fields of the gas above the plane in our model cubes. The results are shown in the lower panels of Fig. 5. Clearly the inclusion of gas accretion changes the direction of the clouds' flow from outflow (bottom panel, pure fountain) to inflow (middle panel, pure fountain).

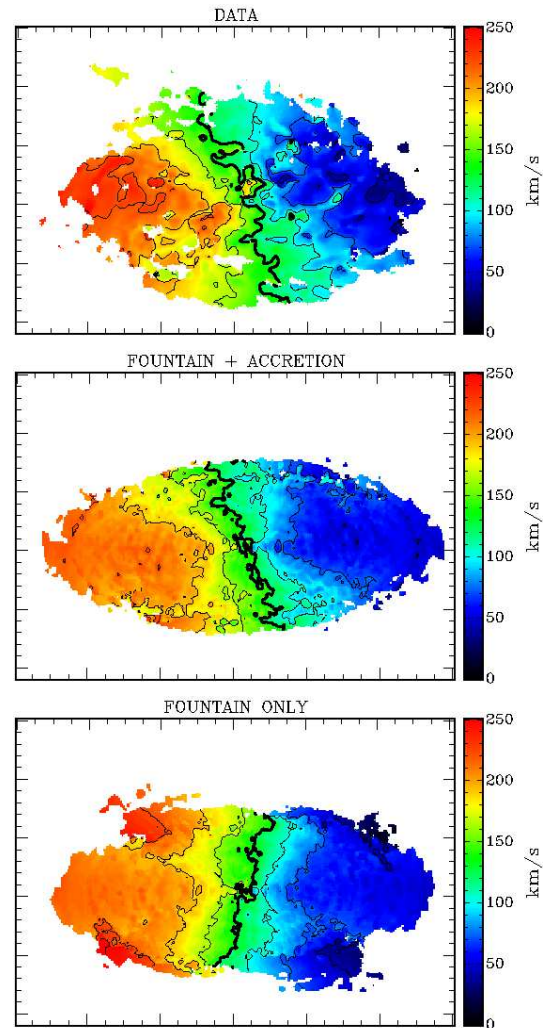


Figure 5. Velocity field for the extra-planar (halo) gas of NGC 2403 (upper panel) (see Fraternali et al. 2001) compared with the two models of fountain + accretion (middle panel) and fountain only (bottom panel). The velocity fields are rotated with the major axis of the galaxy along the horizontal axis. The tilt in the kinematic minor axis is the signature of inflow/outflow.

tilt of the minor axis in the model is also quantitatively very similar to the tilt seen in the data.

The above results occur because the orbits of fountain particles are significantly changed by their interactions with infalling gas; in Fig. 6 the top left and middle left panels show the orbit of a representative particle that is launched at $\sim 60 \text{ km s}^{-1}$ from $R \simeq 5 \text{ kpc}$ in the pure fountain model (top) and the model with infall (middle; notice the different horizontal scales in the two panels). In general the inclusion of accretion makes fountain clouds fall back to the disc at radii that are roughly the same as (or lower than) the starting radii, rather than at larger radii as in classical fountain models (e.g. Collins, Benjamin & Rand 2002). The bottom two panels of Fig. 6 show how in the presence of infall the particle increases in mass and loses specific angular momentum as a result of interactions.

The same accretion model (with the same accretion parameter) is able to produce both the amount of lag of the

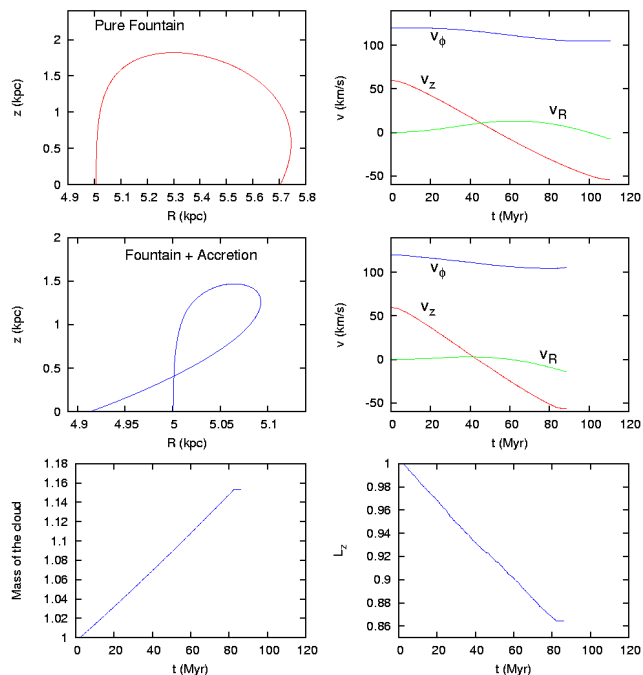


Figure 6. Trajectories of a representative particle in the potential of NGC 2403. The upper panels show the case of a pure fountain, the middle panels show the effect of interaction with accreting material. In the bottom panel we show the modification of the mass and angular momentum of the fountain cloud as a consequence of this interaction.

extra-planar gas in NGC 891 and the inflow pattern required by NGC 2403. Qualitatively it is clear that when fountain particles interact with the accreting material, they both have to share their angular momentum and acquire an inward motion. However, it is remarkable that these effects are made quantitatively correct by a single value of α .

5 RELATION TO OTHER WORK

Our investigation of the coupling between clouds in the HI halo and a corona led to the conclusion that near the plane the corona would rapidly approach corotation with the disc. Galaxies with rapidly spinning, steady-state coronae were investigated by Barnabè et al. (2006). They found that such coronae, taken in isolation, can reproduce the rotation curves shown in Fig. 3, raising the possibility that the observed HI clouds are embedded in and locally at rest with respect to a corona of this type. Because the coronae described by Barnabè et al. enjoy considerable rotational support, they are not very hot: in most of the volume above the disc, $2 \times 10^4 \text{ K} < T < 2 \times 10^5 \text{ K}$. At these temperatures radiative cooling is at peak efficiency, and unless their densities are made extremely low, the cooling times $\sim 1 \text{ kpc}$ above the disc are much shorter than the local dynamical times. Similarly, if densities are not very low, the coronae would be readily detectable in UV emission lines of ions such as O VI.

A second model that has recently been used to fit the rotation curves above the plane of NGC 891 is based on cosmological inflow (Kaufmann et al. 2006). In this model the gas is initially at the virial temperature and spinning. In a

nearly spherical region of radius $\sim 10 \text{ kpc}$ the gas rapidly cools and collapses into the centre. Gas with low angular momentum moves in parallel to the spin axis to take its place, causing the temperature to rise as one approaches the axis at fixed z . Over several Gyr the remaining gas cools onto an annular region of the disc. At this stage the cooling gas lags the rotation of the disc in a manner similar to that observed in NGC 891. In fact, cooling from the initial conditions postulated by Kaufmann et al. (2006) has created a rapidly spinning corona similar to that discussed by Barnabè et al. (2006).

Kaufmann et al. (2006) argue that the cooling corona will spawn clouds of neutral HI that constitute the observed HI halo of NGC 891. Their simulations provide some support for this conjecture, and they argue that the proposal is supported by the analytic work of Maller & Bullock (2006). Since the simulations are subject to numerical artifacts associated with their finite resolution in mass and distance (Kaufmann et al. 2007), the analytic arguments for the existence of cool clouds are important.

We believe that these analytic arguments are flawed because they ignore the ability of a gravitational field to prevent a stratified atmosphere from suffering the Field (1965) thermal instability (Malagoli, Rosner & Bodo 1987; Balbus & Soker 1989).¹ Physically, when an atmosphere is confined by a gravitational field (which can be taken to include the pseudo-field associated with spin), the gas settles on a dynamical time into a stratified configuration, in which the material of lowest specific entropy lies at the lowest potential. In this configuration an overdense region is a region in which the surfaces of constant specific entropy have been perturbed upwards. Consequently it is the crest of an internal gravity wave. On a timescale that is only slightly longer than the dynamical time, the overdensity sinks from lack of buoyancy, overshoots its point of equilibrium, and is soon an underdense region. Consequently the basis of the Field instability – the increase in cooling rate with increased density – cancels out to first order as initially overdense regions oscillate vertically and are on average neither more nor less dense than undisturbed material at their mean position (Balbus & Soker 1989). There is no reason to suppose that hot gas that is cooling onto the disc of a galaxy is more liable to the Field instability than is the gas of cooling flows, which X-ray spectra showed do not evolve according to the Field instability (Peterson et al. 2002), as Malagoli, Rosner & Bodo (1987) predicted more than a decade earlier.

A second problem with the contention that HI haloes represent material that is condensing out of the corona is the massiveness of haloes. In NGC 891, the HI mass detected above 1 kpc from the plane is $1.2 \times 10^9 M_\odot$, almost 30% of the total HI mass (Oosterloo, Fraternali & Sancisi 2007). If this gas were falling towards the disk even at a relatively low speed of $\sim 100 \text{ km s}^{-1}$, taking a mean distance from the plane of about 4 kpc , it would imply an accretion rate of $\sim 30 M_\odot \text{ yr}^{-1}$. Not only does this rate substantially exceed

¹ In Maller & Bullock (2006) the analysis relies on Balbus (1986). However in their equation (20) they misquote Balbus’s equation (5) by misidentifying $\mathcal{L}(T, \rho)$ as the conventional cooling function $\Lambda(T)$.

the current SFR, but it implies that we live in a time when the disc is growing much faster than it has in the past, which is a priori implausible and probably inconsistent with the measured colours of the stellar disc.

Thirdly, Rand & Benjamin (2008) searched for HI around the only spiral galaxy that is known to have a large corona, the edge-on galaxy NGC 5746. Their finding that there is very little HI in the corona is hard to reconcile with the contention of Kaufmann et al. (2006) that thermal instability of coronae leads to the abundant formation of HI clouds.

Finally, from an observational point of view there is strong evidence that a large fraction of the extra-planar gas is indeed produced by the galactic fountain. The distribution of the extra-planar HI in NGC 891 and NGC 2403 is concentrated very close to the star-forming disk and almost absent above and below the outer disk. In other galaxies like NGC 6946 (Boomsma 2007) most of the high-velocity features are located in the inner star forming disc. Moreover, Heald et al. (2007) found that in three galaxies with extra-planar ionised gas, the thickness of the ionised halo as well as the vertical rotational gradient both clearly correlate with the SFRs, pointing to a dominance of the fountain in the formation of these haloes.

6 DISCUSSION AND CONCLUSIONS

Standard cosmology teaches that the majority of the baryons lie somewhere in extragalactic space, probably in a hot diffuse medium. We cannot hope to have an adequate knowledge of the formation and evolution of galaxies until we have a better understanding of the connection between star-forming galaxies and extragalactic gas. In this paper we have shown that the existence of HI haloes around star-forming galaxies has profound implications for this vital connection.

It has long been evident that star-forming galaxies must be accreting gas at significant rates. We have modified the ballistic fountain model to include the effects of clouds sweeping up material that has low angular momentum about the disc's spin axis. The key parameter of the model is the rate α at which the mass of a cloud exponentiates as a result of accretion. We find that a single value, $\alpha \approx 1.5 \text{ Gyr}^{-1}$ enables us to resolve the problems encountered in FB06 with both the edge-on galaxy NGC 891 and the inclined galaxy NGC 2403. Specifically, adding swept-up gas doubles the lag in rotation of the halo with respect to the disc because clouds have to share their angular momentum with swept-up gas, and the any inward motion of accreted material causes the net motion of the fountain gas to be inwards rather than outwards. The aggregate infall rates implied for NGC 891 and NGC 2403 are ~ 2.9 and $\sim 0.8 M_{\odot} \text{ yr}^{-1}$, respectively. These rates are very close to the rates at which star formation is consuming gas in the two galaxies, but $1/5 - 1/10$ of the rates at which star-formation cycles gas through the halo (FB06). This means that most of the neutral gas that we observe in the halo ($\sim 90\%$ in NGC 891 and $\sim 80 - 85\%$ in NGC 2403) is gas that stellar feedback has pushed up from the disc and only a small fraction is accreted. Notably, the obtained accretion rates are not only consistent with the respective SFRs, but also with

the expected cosmological accretion rates for these types of galaxies (e.g. Neistein & Dekel 2008).

It is unclear whether the swept-up gas arises from cooling of a hot medium, or from the infall of cold streams of gas (Birnbom & Dekel 2003; Binney 2004; Keres et al. 2005; Cattaneo et al. 2006), but the long cooling time of coronal gas strongly suggests that it comes from cold streams. The accretion rates onto nearby spiral galaxies determined here are cosmologically significant: if the two galaxies had accreted at their current rates for a Hubble time, they would have added $\sim 1/2 - 1/3$ of their current masses. Hence our estimates are consistent with past accretion rates being larger, but not much larger unless SN feedback is efficient in ejecting material back to the IGM. Note that estimated accretion rates could be considered as lower limits because gas can reach the discs without encountering fountain clouds, either by slipping past these clouds if they have a small filling factor, or by joining the disc at large radii, outside the star-forming region.

The accretion rates estimated here exclude stars brought in by satellites, but since accreted stars cannot contribute to the thin disc, the bulk of the accretion onto these disc-dominated galaxies must be gaseous, consistent with the significant rates of gas accretion that we require.

We have argued that feedback from star formation is essential for the formation of HI haloes – the latter cannot form directly from cooling coronal gas because (i) the latter is not thermally unstable, (ii) if HI haloes represented material that has condensed from the corona, the accretion rate of the thin disc would be implausibly large, and (iii) there is broad observational evidence of a link between galactic fountains and extra-planar gas features.

In the likely event that coronal gas is not swept up by fountain clouds, the corona must be profoundly influenced by interaction with fountain gas. In particular, just above the disc interaction with halo clouds will ensure that the corona is nearly corotating. If the nearly corotating gas is confined near the disc, it must be quite cool ($T \sim 10^5 \text{ K}$) and strongly radiating in the UV. It seems more likely that the corona is hotter and therefore not bound to the vicinity of the disc: then it will flow outwards and upwards.

We have to expect that the interface between HI in a galactic disc and coronal gas is at least as complex and dynamic as that between the solar photosphere and corona because similar physics is at work: global rotation, local vortices, a steep density gradient, upswelling of material, magnetic loops and optically-thin radiative cooling in the temperature range $10^4 - 10^7 \text{ K}$. It is worth noting that above the Sun the transition from $T = 3 \times 10^4 \text{ K}$ to $T = 3 \times 10^5 \text{ K}$ is complete within only $\sim 30 \text{ km}$ (Jordan 1977).

Our assumption that swept-up gas has low angular momentum about the disc's spin axis is both essential and at first sight surprising. Indeed, discs must be formed by gaseous infall, and they are expected to form from inside out as a result of the mean angular momentum of infalling material rising over time. Galaxies such as NGC 4550, which has two counter-rotating stellar discs (Rubin, Graham & Kenney 1992) and the numerous decoupled gaseous/stellar systems found with SAURON (Sarzi et al. 2006) make it certain that whatever may be true of the time-evolution of the magnitude of the specific angular-momentum vector \vec{L} of infalling gas, any given com-

ponent L_z can diminish and even change sign. For our model it is essential only that at the radius R of accretion to a disc with circular speed v_c we have $L_z < \frac{1}{2}Rv_c$. The perpendicular components of \vec{L} could well make $|\vec{L}| > Rv_c$. In the future, it will be possible to test these predictions with hydrodynamical cosmological simulations. Existing models seem to agree qualitatively with our requirements (e.g. Porciani, Dekel & Hoffman 2002).

Moreover, one interpretation of warps in HI discs relies precisely on \vec{L} for infalling material being comparable in magnitude to, but strongly misaligned with, \vec{L} for the outer disc (Ostriker & Binney 1989; Jiang & Binney 1999; Shen & Sellwood 2006). This argument indicates that there could be a connection between disc warping and rotational lag of the HI halo. Interestingly, both NGC 891 and NGC 2403 do show warping of the outer discs (García-Ruiz, Sancisi & Kuijken 2002; Fraternali et al. 2002). However, if the specific angular momentum of infalling material is large enough, there could be negligible infall in the vicinity of the fountain gas. Then the galaxy would have a warped HI disc but an HI halo with only a small rotational lag.

We have modelled the ambient gas as smooth, so fountain clouds receive a constant amount of mass and momentum per given time. In reality, an accretion flow is probably clumpy. However, as long as the gas mass of the accreting clouds is lower than the mass resolution in the data (about $10^6 M_\odot$), no significant difference is expected. For larger accreted masses, the effects of accretion will be more pronounced in some regions of the halo than in others, unless large gas complexes break into smaller clumps, which can be modelled by smooth accretion.

It would be interesting to extend this work to other galaxies, in particular low surface-brightness (LSB) galaxies with low star formation rates that also have HI haloes – UGC 7321 (Uson & Matthews 2003) is an example of such a system. This would allow us to establish if accretion is a common process at the current epoch, and what role it plays in triggering star formation. We are also applying the model to the Milky Way; this work will clarify the relation between fountain gas and the classical phenomena of intermediate- and high-velocity clouds (Fraternali & Binney, in prep.).

ACKNOWLEDGMENTS

This work was in part supported by Merton College, Oxford.

REFERENCES

- Aubert, D., Pichon, C., Colombi, S., 2004, MNRAS, 352, 376
- Balbus S.A., 1986, ApJ, 303, L79
- Balbus S.A., Soker N., 1989, ApJ, 341, 611
- Barnabè M., Ciotti L., Fraternali F., Sancisi R., 2006, A&A, 446, 61
- Benjamin, R.A., Danly, L., 1997, ApJ, 481, 764
- Binney, J., Dehnen, W., Bertelli, G., 2000, MNRAS 318, 658
- Binney J., 2004, MNRAS, 347, 1093
- Birnbom Y., Dekel A. 2003, MNRAS, 345, 349
- Bond, J. R., Cole, S., Efstathiou, G., & Kaiser, N. 1991, ApJ, 379, 440
- Boomsma R. 2007, *PhD Thesis*, University of Groningen
- Bregman, J.N., Houck, J.C. 1997, ApJ, 485, 159
- Brüms, C., Kerp, J., Pagels, A., A&A, 370, L26
- Cattaneo A., Dekel A., Devriendt J., Guiderdoni B., Blaizot J., 2006, MNRAS, 370, 1651
- Collins J.A., Benjamin R.A., Rand R.J., 2002, ApJ, 578, 98
- Dehnen W., Binney J., 1998, MNRAS, 294, 429
- Dekel A., Birnboim Y., 2006, MNRAS, 368, 2
- Field G.B., 1965, ApJ, 142, 531
- Fraternali F., Oosterloo T., Sancisi R., van Moorsel G., 2001, ApJ, 562, 47
- Fraternali F., van Moorsel G., Sancisi R., Oosterloo T., 2002, AJ, 123, 3124
- Fraternali F., Oosterloo T., Sancisi R., Swaters R., 2005, in “Extra-planar Gas”, Dwingeloo, ASP Conf. Series, 331, 239, ed. R. Braun
- Fraternali F. & Binney J.J., 2006, MNRAS, 366, 449 (FB06)
- Fraternali F., Binney J.J., Oosterloo T., Sancisi R. 2007, in “The Fate of Gas in Galaxies”, NewAR, 51, 95, eds. Morganti, Oosterloo, Villar-Martin & van Gorkom
- García-Ruiz I., Sancisi R., Kuijken K. 2002, A&A, 394, 769
- Heald G.H., Rand R.J., Benjamin R.A., Bershady M.A. 2007, ApJ, 663, 933
- Jiang I.-G., Binney J., 1999, MNRAS, 303, L7
- Jordan C., 1977, in *Illustrated Glossary for Solar and Solar-Terrestrial Physics*, eds. A. Bruzek & C.J. Durrant (Reidel: Dordrecht)
- Kaufmann, T., Mayer, L., Wadsley, J., Stadel, J., Moore, B. 2006, MNRAS, 370, 1612
- Kaufmann, T., Mayer, L., Wadsley, J., Stadel, J., Moore, B. 2007, MNRAS, 375, 53
- Kennicutt R.C. Jr., Armus L., Bendo G., Calzetti D., Dale D.A., Draine B.T., Engelbracht C.W., Gordon K.D., Grauer A.D., Helou G., Hollenbach D.J., Jarrett T.H., Kewley L.J., Leitherer C., Li A., Malhotra S., Regan M.W., Rieke G.H., Rieke M.J., Roussel H., Smith J.-D.T., Thornley M.D., Walter F., 2003, PASP, 115, 928
- Keres, D., Katz, N., Weinberg, D.H., Davé, R., MNRAS, 363, 2
- Knebe A., Gill S.P.D., Gibson B.K., Lewis G.F., Ibata R.A., Dopita M.A., ApJ, 603, 7
- Lacey, C., Cole, S., 1993, MNRAS, 262, 627
- Lacey, C.G., Ostriker, J.P., 1985, ApJ, 229, 633
- Liedahl D.A., Osterheld A.L., Goldstein W.H., 1995, ApJL, 438, 115
- Mac Low M.-M., Ferrara A. 1999, ApJ, 513, 142
- Malagoli A., Rosner R., Bodo G., 1987, ApJ, 319, 632
- Maller, A.H., Bullock J.S., 2004, MNRAS, 355, 694
- Matteucci, F., 2003, in “Origin and Evolution of the Elements”, ed. A. McWilliam & M. Rauch (Cambridge: Cambridge University Press) (astro-ph/0306034)
- Matthews L.D., Wood K., 2003, ApJ, 593, 721
- Mewe R., Lemen J.R., van den Oord G.H.J., 1986, A&AS, 65, 511
- Neistein E., Dekel A. 2008, MNRAS, 383, 615
- Oosterloo T., Fraternali F., Sancisi R., 2007, AJ, in press
- Ostriker E.C., Binney J.J., 1989, MNRAS, 237, 785
- Pedersen, K., Rasmussen, J., Sommer-Larsen, J., Toft, S.,

- Benson, A.J., Bower, R.G., 2006, *New Astron.*, 11, 465
- Peek J.E.G., Putman M.E., Sommer-Larsen J. 2007, *ApJ*, in press
- Peterson J.R., Kahn S.M., Paerels F.B.S., Kaastra J.S., Tamura T., Bleeker J.A.M., Ferrigno C., Jernigan J.G., 2003, *ApJ*, 590, 207
- Popescu C.C., Tuffs R.J., Kylafis N.D., Madore B.F., 2004, *A&A*, 414, 45
- Porciani C., Dekel A., Hoffman Y. 2002, *MNRAS*, 332, 325
- Quinn, T., Binney, J., 1992, *MNRAS*, 255, 729
- Rand R.J., Benjamin R.A., 2008, arXiv0801.1069
- Rubin V.C., Graham J.A., Kenney J.D.P., 1992, *ApJ*, 394, L9
- Sancisi R., Fraternali F., Oosterloo T., van der Hulst J.M. 2008, *A&ARv*, in press
- Sarzi, M., Falcn-Barroso, J., Davies, R.L., Bacon, R., Bureau, M., Cappellari, M., de Zeeuw, P.T., Emsellem, E., Fathi, K., Krajnovi, D., Kuntschner, H., McDermid, R.M., Peletier, R.F. 2006, *MNRAS*, 366, 1151
- Semelin, B., Combes, F., 2005, *A&A*, 441, 55
- Shen J., Sellwood J.A., 2006, *MNRAS*, 370, 2
- Sommer-Larsen, J. 2006, *ApJ*, 644L, 1
- Spitzer, L., 1956, *ApJ*, 124, 20
- Strickland, D.K., Heckman T.M., Colbert E.J.M., Hoopes C.G., Weaver K.A., 2004, *ApJS*, 151, 193
- Swaters R.A., Sancisi R., van der Hulst J.M., 1997, *ApJ*, 491, 140
- Tinsley, B.M., 1981, *ApJ*, 250, 758
- Toth, G., Ostriker, J.P., 1992, *ApJ*, 389, 5
- Tripp T.M., Wakker B.P., Jenkins E.B., Bowers C.W., Danks A.C., Green R.F., Heap S.R., Joseph C.L., Kaiser M.E., Linsky J.L., Woodgate B.E., 2003, *AJ*, 125, 3122
- Twarog, B.A., 1980, *ApJ*, 242, 242
- Uson J. M., Matthews L. D. 2003, *AJ*, 125, 2455
- van der Hulst J.M. & Sancisi R. 1988, *AJ*, 95, 1354
- van der Hulst J.M. & Sancisi R. 2005, *ASPC*, 331, 139
- Wakker B.P., van Woerden H., 1997, *ARA&A*, 35, 217
- Wakker B.P., York D.G., Howk C., Barentine J.C., Wilhelm R., Peletier R.F., van Woerden H., Beers T.C., Ivezić Z., Richter P., Schwarz U.J. (2007), *ApJ*, 670, 113L
- Wakker B.P., York D.G., Wilhelm R., Barentine J.C., Richter P., Beers T.C., Ivezić Z., Howk J.C. (2008), *ApJ*, in press, (astro-ph/0709.1926)
- Westmeier, T., Braun, R., & Thilker, D. 2005, *A&A*, 436, 101
- White S.D.M., & Frenk C.S. 1991, *ApJ*, 379, 52

This paper has been typeset from a $\text{\TeX}/\text{\LaTeX}$ file prepared by the author.